Contents list available at IJRED website

International Journal of Renewable Energy Development

Journal homepage: https://ijred.undip.ac.id

Research Article

Characterization of plant growth promoting potential of 3D-printed plant microbial fuel cells

Diane Pamela E. Palmero[a] and Kristopher Ray S. Pamintuan[a,b*]

[a]*School of Chemical, Biological. and Materials Engineering and Sciences, Mapua University, Manila, Philippines*

[b]*Center for Renewable Bioenergy Research, Mapua University, Manila, Philippines*

Abstract. Plant-Microbial Fuel Cell (PMFC) is an emerging technology that converts plant waste into electrical energy through rhizodeposition, offering a renewable and sustainable source of energy. Deviating from the traditional PMFC configurations, additive manufacturing was utilized to create intricate and efficient designs using polymer-carbon composites. Concerning the agricultural sector, the effect of 3D-printed PMFCs on the growth and biomass distribution of *Phaseolus lunatus* and *Ipomoea aquatica* was determined. The experiment showed that electrostimulation promoted the average daily leaf number and plant height of both polarized plants, which were statistically proven to be greater than the control ($\alpha = 0.05$), by energizing the flow of ions in the soil, boosting nutrient uptake and metabolism. It also stimulated the growth of roots, increasing the root dry mass of polarized plants by 155.44% and 66.30% for *I. aquatica* and *P. Lunatus* against their non-polarized counterpart. Due to the biofilm formation on the anode surface, the number of root nodules of the polarized *P. lunatus* was 51.30% higher than the control, while the protein content in the PMFC setup was 42.22% and 8.26% higher than the control for *I. aquatica* and *P. lunatus*, respectively. The voltage readings resemble the plants' average growth rate, and the polarization studies showed that the optimum external resistances in the *I. aquatica*- and *P. lunatus*-powered PMFC were 4.7 kΩ and 10 kΩ, respectively. Due to other prevailing pathways of organic carbon consumption, such as methanogenesis, the effect of polarization on the organic carbon content in soil is currently inconclusive and requires further study.

Keywords: 3D-printed electrodes, electricity generation, organic carbon, plant growth, plant-microbial fuel cell, protein, root nodules

Received: 4th Feb 2023; Revised: 25th June 2023; Accepted: 7th July 2023; Available online: 28th July 2023

1. Introduction

Plant-Microbial Fuel Cell (PMFC) is an emerging bioelectrochemical technology that converts the stored chemical energy in plants to electrical energy (Imbrogno et al. 2019). Through photosynthesis, plants produce rhizodeposits that serve as the substrate for the electroactive microorganisms in the rhizosphere (Narayana Prasad and Kalla 2021). These microorganisms release electrons that generate electricity (Zhou *et al.* 2022). An innovative method for producing materials for fuel cells is additive manufacturing. It was initiated in 2018 (Kamali *et al.* 2023) and has been applied to various electrochemistry applications for its resource efficiency and cost-effectiveness (Peng *et al.* 2018). Conductive polymer-carbon composites are common materials for 3D-printing electrodes that are known for having high anisotropic conductivity, more electroactive sites, and low resistivity (Omar *et al.* 2021). However, the presence of polymer causes low surface area, but it can be easily solved by designing 3D models with higher surface area (You *et al.* 2017). Concerning the agricultural sector, it is essential to characterize the effects of such systems on the growth of plants.

Recent studies have shown various ways to optimize the cost-effectiveness of PMFC for the prospects of large-scale applications. Different configurations, environmental conditions, and applications concurrent with electricity generation were discussed (Kabutey *et al.* 2019)(Narayana Prasad and Kalla 2021). Also, the performance of different types of ceramics as membranes in MFCs was explored and characterized (Winfield et al. 2016)(Sarma and Mohanty 2023). The progressive research on PMFC leads to the unraveling of more factors and aspects that must be considered. These include standardization and geographical optimization barriers due to a lack of data for analysis (Maddalwar *et al.* 2021). Studies also emphasize that the plant-microbe relationship and characterization of *Rhizodeposits* require further exploration (Nitisoravut and Regmi 2017). Hence, experimentation with plants with higher rhizodeposition is needed (Lu *et al.* 2020). Research on bioelectricity production from food crops was recommended by Arulmani *et al.* (2021). Lastly, the development of more 3D-printed electrode designs is suggested to further improve PMFC performance (Omar et al. 2021).

The main objective of this study is to determine the effect of 3D-printed PMFCs on the growth and biomass distribution of agriculturally valued plants *Phaseolus lunatus* (Lima bean) and *Ipomoea aquatica* (Water spinach). Specifically, it aims to analyze and characterize the growth of plants by measuring the following growth parameters; plant height, number of leaves, dry mass of roots, number of root nodules, protein content of the leaves, and organic carbon content of the soil. This study

* Corresponding author
Email: krspamintuan@mapua.edu.ph (K.R.S. Pamintuan)

https://doi.org/10.14710/ijred.2023.52291
ISSN: 2252-4940/© 2023. The Author(s). Published by CBIORE

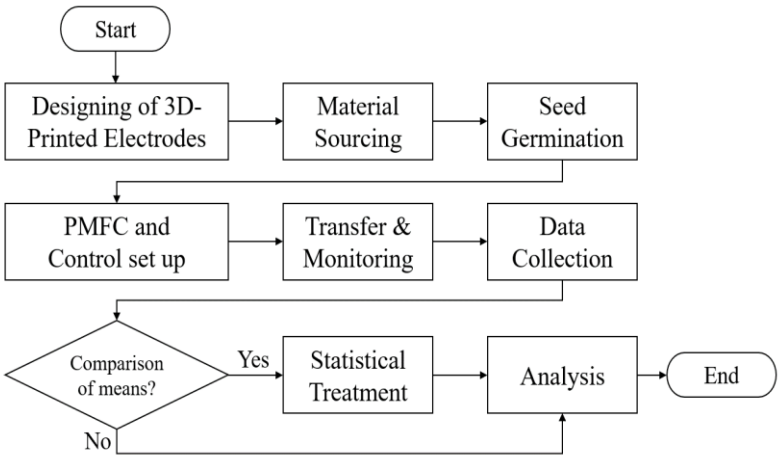

Fig. 1 Methodology Flowchart

could benefit the agricultural and energy sector by simultaneously meeting the rising demand for renewable energy and food supply. The obtained empirical data would support the growth enhancement effect of PMFCs, which could improve farm productivity. At the same time, the electricity generated can be used as a power supply for the farm and the surrounding communities, increasing PMFC scalability.

2. Materials and Methods

The characterization of the effects of bioelectricity production from *P. lunatus* (Lima bean) and *I. aquatica* (Water spinach) on their growth involves several thorough steps, as shown in Fig. 1. Experimental and control setup was conducted to compare the growth parameters.

2.1 Designing of 3D-printed Electrodes

The electrodes were produced through additive manufacturing. It was designed in the Autodesk Fusion 360 software considering the factor of surface area in the performance of PMFC. Both electrodes are hexagonal prism-shaped with a thickness of 2.50 mm. It has triangular holes with a base and height of 2 mm, which allows it to add 15.07 mm^2 of surface area per hole for the anode and 13.07 mm^2 of surface area per hole for the cathode. The 3D model for the anode is shown in Fig. 2a. It has a height of 54 mm and an outside diameter of 52.70 mm. Each side has a length of 26.35 mm and 204 triangular holes. As shown in Fig. 2b, the cathode has a height of 73 mm, an outside diameter of 34 mm, and an inside diameter of 28.23 mm. Each inner side has a length of 14.11 mm and 192 triangular holes. It also has fins having the same height, 3 mm length, and 0.50 mm thickness, directed inwards to increase the cathode surface area further. The outer surface area of the anode is 26,983.08 mm^2, while the total surface area of the cathode is 36,568.13 mm^2 having a cathode-to-anode surface area ratio of 1.36.

2.2 Material Selection

The materials used for each component of the PMFC are shown in Table 1. The plastic pots were sourced from a local supplier from Victoria, Laguna, while the copper wires were from Quezon City, Metro Manila. The Proto-pasta electrically conductive composite PLA was directly bought from ProtoPlant, USA. The Terracotta membranes were obtained from a supplier in China. Lastly, the plant seeds were procured from commercial seed suppliers in the Philippines.

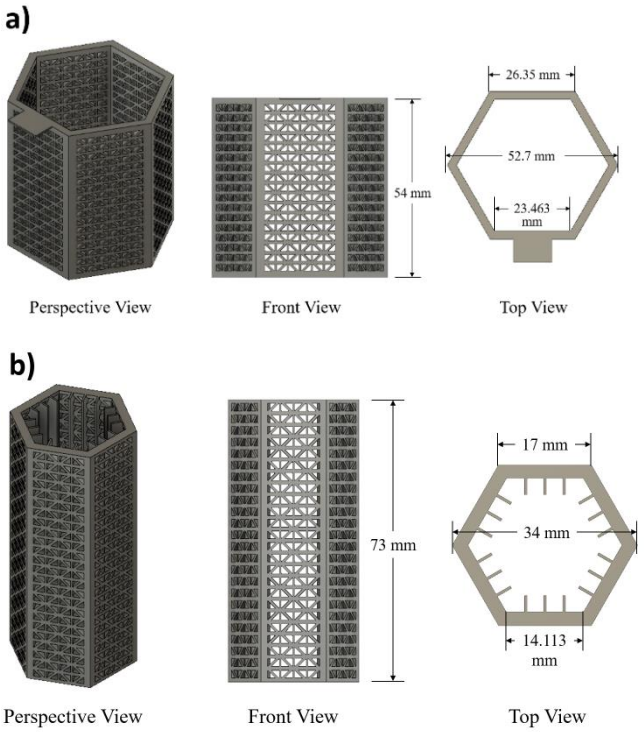

Fig. 2 Perspective, Front, and Top view of (a) Anode and (b) Cathode 3D Models

Table 1
Materials used in PMFC

Component	Material
PMFC Exterior	Plastic pot
Anode	Conductive PLA
Cathode	Conductive PLA
Membrane	Terracota
Growing medium	Soil
Wire	Copper

2.3 Seed Germination

The seeds were not planted directly on the PMFC setup and was germinated first in three-by-four propagation trays with dimensions of 160-mm × 115-mm × 55-mm (L × W × H). It has holes at the bottom for water drainage and a transparent plastic cover with adjustable humidity vents. For the *I. aquatica* (water

spinach), the seeds were soaked in water for 24 hours before the germination process. The germination process was conducted outdoors. The seeds were planted 1 inch deep in the soil and then left to germinate for twenty days. In that time span, the plants were watered and exposed to eight to ten hours of sunlight on a daily basis.

2.4 PMFC and control setup

The setup of PMFC in this study is shown in Fig. 3a. The exterior of the single-chambered PMFC is a conventional plastic plant pot having the dimensions 210-mm × 145-mm × 190-mm (D_1 × D_2 × H) with drainage holes at the bottom. Each 3D-printed electrode with a terracotta membrane was individually placed in a plastic pot in the middle of two plants of the same kind. This is to mimic its behavior in a stacked PMFC setup, but the effect on the plants can be measured in terms of a single PMFC only. Copper wires were attached to the electrodes for the voltage and current measurement.

Fig. 3b shows the arrangement and dimensions of the electrodes and the membrane. The anode is located in the outermost part so that it is readily available for interaction with the roots wherein the microorganisms are present. In the middle is the stake-type terracotta separator. Due to its high porosity, it readily absorbs moisture and served as the passage for the hydrogen ions or protons to the cathodic region. The stake-type design allows the membrane to be easily pushed and inserted into the soil. Lastly, in the innermost part is the cathode, wherein the hydrogen ion reacts with oxygen to form water.

There are two control setups for this experiment, a soil PMFC with no plant (Fig. 4a) and plants with no PMFC (Fig. 4b). The first one was the basis for comparison of the growth enhancement provided by the PMFC, while the latter was used to measure the baseline power generation of the soil used in the experiment. There are four trials for *I. aquatica* and its control, three trials for *P. lunatus* and its control, and one setup for the plantless soil PMFC, having a total of seven PMFC setups and eight control setups.

2.5 Transfer & Monitoring

Upon seed germination, the plants were transferred to their respective PMFC and control setups. It was ensured that their roots are completely covered with soil for optimal nutrient access. Before the data collection, a ten-day downtime was allotted for the plants to adapt to their new environmental condition, accompanied by consistent supervision and hydration. A fixed volume of tap water was used to water the plants daily.

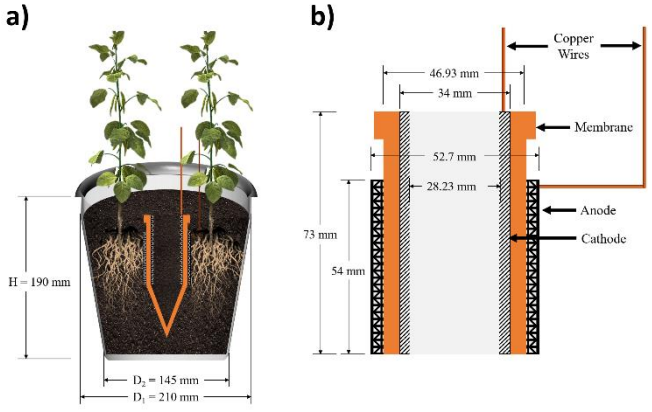

Fig. 3 (a) PMFC setup and (b) electrode arrangement

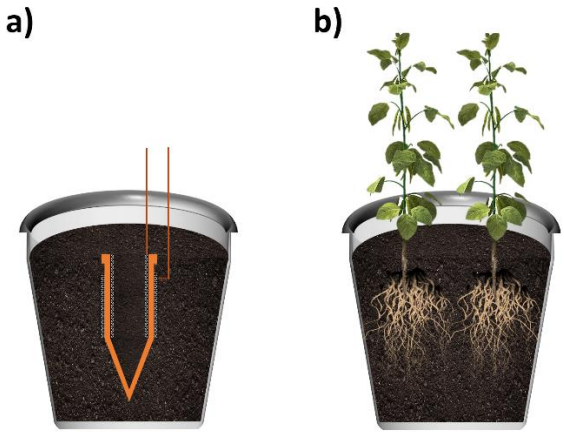

Fig. 4 (a) Soil- and (b) plant-control setup

2.6 Data Collection

Voltage and current measurements were conducted every 9:00 AM for fifty consecutive days using a digital multimeter (UNI-T UT60BT). The growth parameters, namely plant height and root dry mass, were measured using a steel tape measure and analytical balance, respectively. Whereas the leaf number and root nodules were manually counted. Chemical analyses were also conducted to determine the nutrient content in leaves and soil. Protein content analysis was conducted in leaf samples using the Kjeldahl method, and the organic carbon content analysis was conducted in soil samples using Titrimetry (Walkey-Black). These analyses were performed by the Sentro sa Pagsusuri, Pagsasanay, at Pangangasiwang Pang-agham at Teknolohiya (SentroTek) laboratory.

Various growing conditions of the plant are also measured. The soil's pH and temperature were measured using a digital soil tester. The ambient temperature and humidity were measured using the Xiaomi Mijia Thermometer/Hygrometer with Sensirion sensor. Lastly, polarization was conducted on the last day of data collection. Voltage and current were measured against resistors ranging from 1 Ω to 1 MΩ to optimize power generation. Table 2 presents the equations used to calculate the current (I), power (P), and power density (PD) of the system, where V represents voltage, R represents resistance, and A_S represents the surface area of the anode. These parameters are crucial in understanding the electrochemical properties of the system under study and are defined in the table for reference.

2.7 Data Analysis

A one-tailed paired differences T-test was used in this study to compare the average daily plant height and leaf number of the experimental and control setup of *P. lunatus* (Lima Bean) and *I. aquatica* (Water Spinach), given that the data is time series. The tests made use of a significance level of 0.05, wherein the null hypothesis is that the difference between the average growth parameters of the experimental setup and the control setup ($d = \mu_P - \mu_C$) is less than or equal to zero ($d \leq 0$), while the alternative hypothesis is that the difference is greater than zero

Table 2
Formulas for data collection

Parameter	Equation
Current	I = V / R
Power	P = I ×V
Power Density	PD = P / A_S

(d > 0), indicating that the average growth parameters of the experimental setup are greater than the control setup. For the remaining growth parameters, the arithmetic mean and standard deviation were used.

The data collected were analyzed through different graphical representations. The average daily voltage readings were plotted against time throughout the 50 days of the experiment to observe the behavior of voltage changes. The maximum power density obtained was compared with previous studies that utilized 3D-printed PMFCs. The average final plant height, leaf number, root dry mass, number of root nodules, protein content of leaves, and organic carbon content of soil were presented in bar graphs for a side-by-side comparison. The average growth rate was also calculated and analyzed alongside the average daily voltage readings. Lastly, a polarization curve (Power Density vs. Current Density plot) was produced from the measurement in polarization studies to determine the optimum resistor value for the process.

3. Results and Discussion

3.1 Performance of 3D-printed Electrodes

The surface resistances along the length of the 3D-printed electrodes used in this study are shown in Fig. 5. The average resistance of the dry anode is 1.15 kΩ, while the dry cathode is 1.26 kΩ. As the electrodes were soaked in water for 24 hours, the average resistance slightly increased to 1.35 kΩ and 1.40 kΩ for the anode and cathode, respectively. After being used up in the experiment proper, which took place for 58 days, the electrodes had minimal degradation and fouling, as shown in Fig. 6. Corrosion is more evident in the cathode, which could have resulted from being consistently submerged underwater. Previous studies observed an increase in internal resistance and a decrease in the performance of the PMFC due to cathode fouling (Gude 2016)(Jyoti Sarma and Mohanty 2022), which is similar with the findings of this study, having a 3.7-fold and 12-fold increase in the average surface resistances for the anode and cathode, respectively.

In modeling studies of PMFC performance and behavior, the electrode resistance is often neglected in the internal resistance as it has a minimal value, especially the traditional fuel cells that use pure carbon materials for electrodes (Karamzadeh et al. 2020). Therefore, it was perceived to have minimal impact on the overall performance of PMFC. However, 3D-printed electrodes are composites containing non-conductive polymers, such as PLA, resulting in a slightly higher resistance, which contributes to the overall internal resistance of the PMFC. Internal resistance is considered one of the challenges faced by

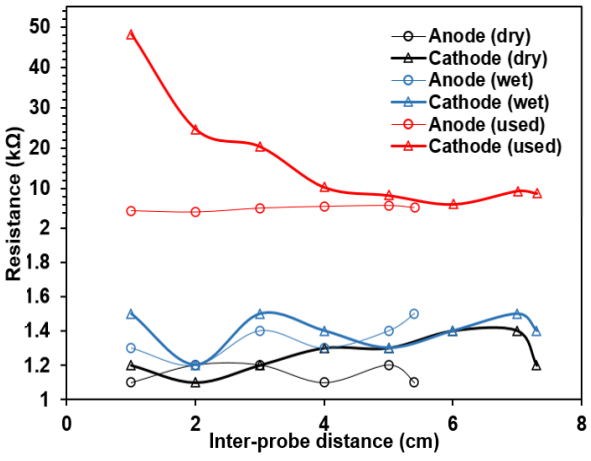

Fig. 5 Surface resistance of 3D-printed electrodes

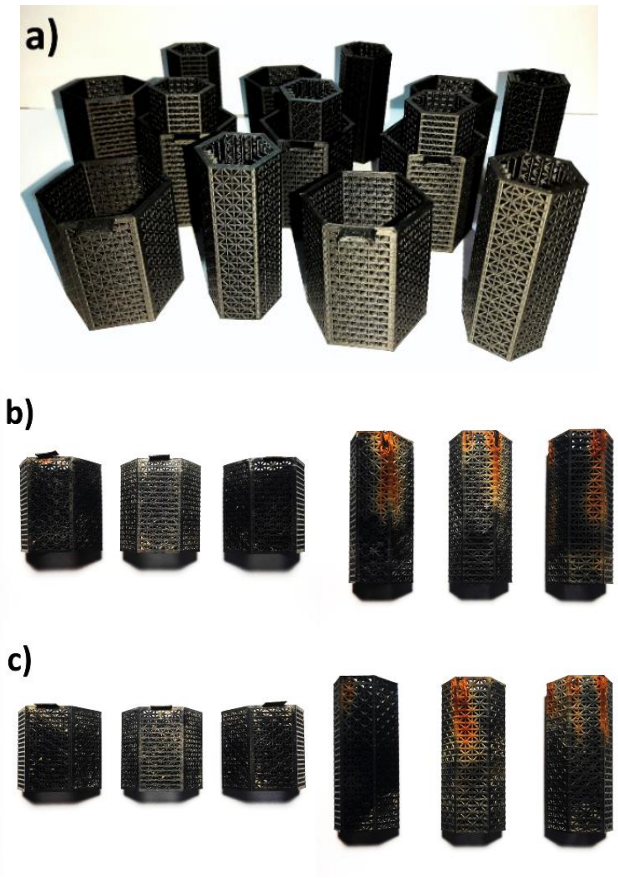

Fig. 6 3D-printed anodes and cathodes (a) before the experiment, (b) after usage in WS-PMFC, and (c) after usage in LB-PMFC

utilizing 3D-printed electrodes, resulting in reduced conductivity (Huang et al. 2021). It is crucial to overcome this disadvantage, which could be done by optimizing the trade-off between electron transfer and internal resistance and incorporating other available 3D-printing filaments and methods of printing.

The 3D-printed electrodes used in this study, which are made of a cost-effective and widely available PLA/Carbon black filament (Rocha et al. 2022), obtained a comparable maximum power density to other similar studies that also made use of 3D-printed fuel cell components. The feedstock, material used for the 3D-printed component, and maximum power or power density of different studies were summarized in Table 3. The maximum power or power density obtained in this study was higher than those studies that utilized the same material (i.e., PLA-carbon composite filaments) for the 3D-printed electrodes (You et al. 2017)(Slate et al. 2021). Therefore, the design of the electrode developed in the study was more effective in power generation. Moreover, the study with the highest maximum power density was reasonable; despite using non-conductive PLA, it underwent a carbonization process wherein it was double-coated with carbon. Hence, its surface's biocompatibility and conductivity were increased (You et al., 2020).

3.2 Plant shoot and root biomass

From the time series plots for the average leaf number (Fig. 7), it was found that the difference in the average leaf number between polarized and non-polarized samples of *I. aquatica* (Fig. 7a) showed more fluctuating behavior along the duration of the experiment than the *P. lunatus* (Fig. 7b), which is steadier and also higher. The difference has its peak on the 33rd and 43rd

Table 3
Comparison with 3D-printed electrode performances across different MFC systems

Component	Feedstock	Material	Maximum Power/ Power Density
Anode and Cathode	*Pseudomonas aeruginosa*	PLA/graphene (8 wt%)	110.74 ± 14.63 μW m^{-2} [a]
Anode and Cathode	Sewage Sludge enriched with 1% tryptone and 0.5% yeast extract	Carbon-coated non-conductive PLA	376.70 μW (7.50 W m^{-3}) [b]
Anode	*Shewanella oneidensis* MR-1	Copper-coated UV curable resin	6.45 ± 0.50 mW m^{-2} [c]
Anode	Sewage Sludge	Conductive PLA	43 ± 1 μW [d]
Anode and Cathode	Rhizodeposits of *I. aquatica*	Conductive PLA	52.33 μW (1.86 mW m^{-2}) [e]
	Rhizodeposits of *P. lunatus*	Conductive PLA	35.46 μW (1.26 mW m^{-2}) [e]

Source: a Slate et al., (2021), b You et al., (2020), c Bian et al., (2018), d You et al., (2017), e This study (2023)

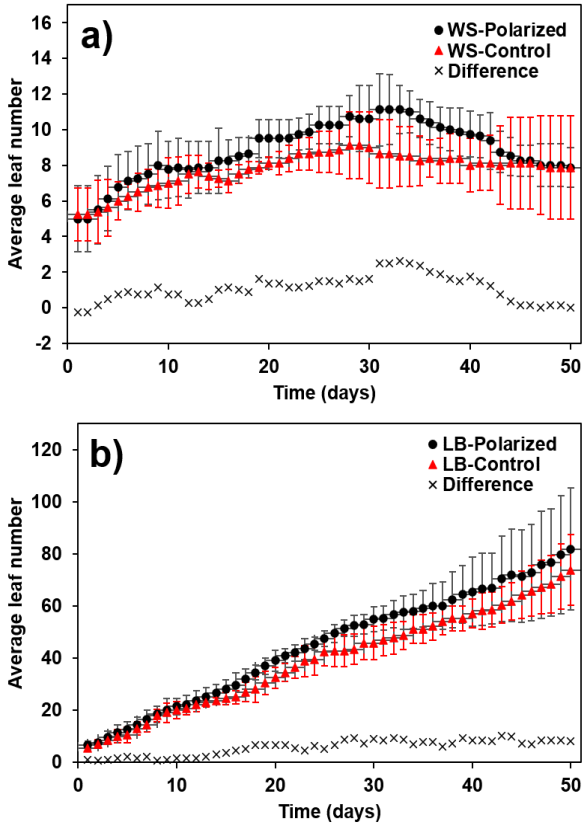

Fig. 7 Average leaf number of (a) *I. aquatica* and (b) *P. lunatus* throughout the 50-day experiment

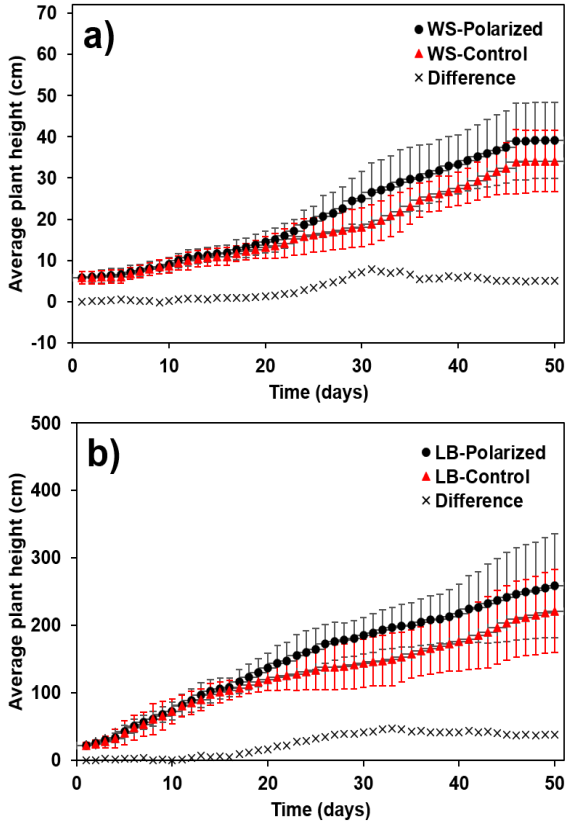

Fig. 8 Average plant height of (a) *I. aquatica* and (b) *P. lunatus* throughout the 50-day experiment

day of the experiment for the *I. aquatica* and *P. lunatus*, respectively. In contrast, the time series plots for the average plant height (Fig. 8) are both steadily increasing. In this parameter, the highest difference for polarized and non-polarized samples of *I. aquatica* is 7.81 cm and for *P. lunatus* is 47.33 cm, which occurred on the 31st and 33rd day of the experiment, respectively. Hence, on average, the polarized plants have a greater number of leaves and grow faster compared to non-polarized plants ($\alpha = 0.05$).

Moreover, it was also observed that the yellowing and wilting of older leaves were immediately exhibited by the polarized and non-polarized *I. aquatica* on the 9th and 5th day of the experiment, respectively. This phenomenon is called leaf senescence, wherein the macromolecules of older leaves, such as proteins, membrane lipids, RNA, and chlorophyll, undergo degradation, resulting in the yellowing of leaves. At the same time, the nutrients are remobilized into the other developing parts of the plant (Kumar *et al.* 2018)(Yamaguchi *et al.* 2010)(Nogué, Gonneau, and Faure 2003).

Leaf senescence can be caused by different factors, such as plant growth regulators (PGRs), reactive oxygen species (ROS), the carbon/nitrogen (C/N) relationship, pathogens, light deprivation, mineral deficiency, seed development, drought, presence of sugars, and ultraviolet and ozone exposure. PGRs or phytohormones regulate the senescence of a plant, ethylene, jasmonic acid, salicylic acid, and abscisic acid induces senescence, while cytokinins, polyamines, nitric oxide, and gibberellin acid inhibits senescence. ROS, namely hydrogen peroxide (H_2O_2), superoxide radical ($O2^{\bullet-}$), and hydroxyl radicals ($OH^{\bullet}$), are responsible for oxidative stress that damages the macromolecules (Shamsi *et al.* 2018)(Lim and Nam 2005)(Kumar *et al.* 2018)(Sharma and Agarwal 2018). On the other hand, the C/N relationship refers to the ratio of carbon and nitrogen content in the soil. An imbalance could result in either acceleration or delay in senescence (He *et al.* 2003).

Table 4
Average final growth parameters of the polarized and control samples of *I. aquatica* and *P. lunatus* at the end of the experiment

Plant	Growth Parameter	PMFC	Control
I. aquatica	Leaf number	8.13 ± 1.25	6.63 ± 1.60
	Plant height (cm)	41.25 ± 7.91	37.38 ± 4.70
	Root dry mass (mg)	85.99 ± 49.10	33.66 ± 8.65
P. lunatus	Leaf number	84.33 ± 26.10	75.50 ± 16.85
	Plant height (cm)	274.50 ± 88.13	232.67 ± 70.66
	Root dry mass (mg)	48.67 ± 21.36	32.17 ± 11.86

The leaf senescence of *I. aquatica* was very early compared to *P. lunatus*, which occurred on the 33rd day of the experiment. This could have resulted from the relatively higher C/N ratio in *I. aquatica*. At elevated CO_2 and low N_2 content, hydrogen peroxide (H_2O_2) production increases, which results in oxidative stress (Agüera and De la Haba 2018), as previously mentioned.

The average final leaf number, plant height, and root dry mass of *I. aquatica* and *P. lunatus* at the end of the experiment were presented in Table 4. The aforementioned characteristics were found to be higher in the polarized plants than in the non-polarized (control) plants on average. Specifically, the average final leaf number, plant height, and root dry mass for the polarized *I. aquatica* is 22.64%, 10.37%, and 155.44% higher than the control, respectively. Whereas for the polarized *P. lunatus*, the average final leaf number, plant height, and root dry mass is 11.70%, 17.98%, and 66.30% higher than the control, respectively. It is also evident from the data that the variation is relatively high in *P. lunatus*. The large variations are characteristic of plant-microbial fuel cells due to the biological nature of the system. Nevertheless, it is still dependent on the characteristic of the plant. This result is in line with the findings of Guan and Yu (2021).

One common cause of growth enhancement in polarized plants is electrostimulation. It is the incorporation of electricity into the plant system, which is known for its ability to regulate plant growth by modifying cellular metabolism, with electric field inducing faster movement of ions in the soil, boosting nutrient uptake and metabolism in the plant (Li, Gou, and Li 2019). It is also being eyed as a replacement for the usual chemical fungicides for plant defense, as it has been proven to reduce fungal diseases in plants (Mori *et al.* 2021). A study on Cucumis sativus using modified electrodes has shown improvements in plant germination, stem thickness, stem and root length, cotyledon length, actual leaf size, biomass, organic matter content, cation exchange capacity, and enzymatic activity (Morales *et al.* 2021).

Different intensities of electric field pulses have varying effects on plants and applications. Very high-intensity electric pulses are used in immobilizing eukaryotic, gram-positive, and gram-negative microorganisms at low temperatures (Wouters *et al.* 1999). Low-intensity electric pulses, on the other hand, was proven by Young Yi *et al.* to cause an increase in the growth of lettuce plant at 4~10 V, growth and fruiting duration as well as the weight of the dried fruits of hot pepper plant, and the enhanced development of roots from cuttings (Yi *et al.* 2012). It also impedes biofilm formation on the electrode as it increases the activity and predominance of certain microorganisms, promoting inoculate microorganism populations (Hoseinzadeh et al. 2020).

Additionally, the carbon black component of the conductive PLA filament could have also contributed to the growth enhancement of polarized plants. Previous researches have shown that the utilization of carbon black fertilizers that are dispersed in bulk soil resulted in higher plants, increased plant shoot (105 – 107%) and root (67 – 70%) biomass yield, and reduced physiological damage (Zhao et al. 2021)(Cheng et al. 2020). Still, it may not be as effective, as the carbon black component of the electrode is only present in small amounts and is immobilized in PLA.

3.3 Nodulation and rhizosphere microbiome

Root nodules are clusters of microbial communities found in the roots of legumes. It is resided by rhizobacteria, which are gram-negative bacteria (Proteobacteria) that conduct nitrogen fixation process that provides nutrients to the plants. It is formed through a regulated process of chemical signals that stimulate the release of flavonoids and chitooligosaccharides between the host plant and the microorganisms in the soil (Yoneyama and Natsume 2010)(Q. Wang, Liu, and Zhu 2018). In this study, the final average number of root nodules is shown in Fig. 9, wherein the PMFC setup has an average of 48.67 ± 21.36, which is 51.30% higher than its control counterpart.

In PMFCs, biofilms are formed on the surface of the anode, which plays a role in electron transfer for electricity generation (Zhou et al. 2022)(Bataillou, Haddour, and Vollaire 2022). Since the roots are near the anode surface, the bacterial communities in the biofilms may have promoted further formation of root nodules. Some bacteria are capable of producing phytohormones (e.g., auxins and cytokinins), which are known for inducing nodule development (Egamberdieva et al. 2017)(Roy Choudhury, Johns, and Pandey 2019). Rhizobial surface polysaccharides, which is an extracellular polymeric substance (EPS) found in biofilms, are essential in the nodulation of some legumes. However, the mechanism is still under investigation (Costa, Raaijmakers, and Kuramae 2018). Moreover, a PCoA based on the Bray–Curtis distances showed that the rhizosphere microbiome including *Comamonadaceae*, *Pseudomonadaceae*, *Alicyclobacillaceae*, *Paenibacillaceae*, *Rhizobiaceae*, *Bacillaceae*, and *Microbacteriaceae* contributed to *Sinorhizobium* nodulation, while *Micrococcaceae*, *Intrasporangiaceae*, *Gaiellales*, and *Saccharibacteria* were correlated to *Bradyrhizobium* nodulation (Han et al. 2020).

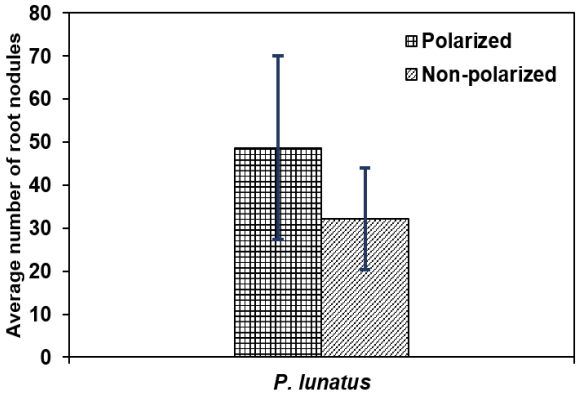

Fig. 9 Average number of root nodules in P. lunatus roots at the end of the experiment

The abundance of microorganisms in the rhizosphere may also be represented through the number of root nodules. Nodulation characteristics such as nodule biomass, nodule number, and nitrogenase activity was found to have contributed by 56.56% to the diversity of rhizosphere microbiome. Specifically, *Bradyrhizobium* were correlated with the nodule number, *Burkholderia* with nodule biomass and nitrogenase activity, and *Dyella* were correlated to all characteristic (H. Wang et al. 2020). With this, it could be inferred that PMFC enhanced the rhizosphere microbiome diversity. Nevertheless, further studies are necessary to strengthen this claim.

3.4 Protein content in leaves

The crude protein content, expressed in weight percentage, in the leaves of *I. aquatica* and *P. lunatus* is shown in Fig. 10. It was found that the protein content in the PMFC setup was 42.22% and 8.26% higher than the control for *I. aquatica* and *P. lunatus*, respectively. Nitrogen-fixing bacteria also play an essential role in increasing the protein content of a plant, resulting in higher protein contents in the leguminous plant. They convert atmospheric nitrogen N_2 into more useful nitrogen nutrients, including nitrate, which is the necessary nutrient for protein synthesis along with glucose. Aside from that, the bacterial community in the biofilm on the surface of the electrode also contributes to protein synthesis. Some microorganisms have the ability to convert the nutrients in the soil, including organic carbon, nitrogen, and phosphorus, into microbial protein (Matassa *et al.* 2016). While others, like H_2-oxidizing bacteria (HOB), make use of hydrogen, oxygen, and carbon dioxide molecules to produce protein (Zhang *et al.* 2020).

Moreover, the application of electric current in plants could also contribute to protein synthesis by altering the activity of enzymes and other proteins involved in the process. A study showed that a 6V DC provided through graphite electrodes enhanced the activity of laccase, an enzyme in plants, in the anode region (C. Wang *et al.* 2015). Most importantly, electrical stimulation also enhances protein synthesis by inducing plant defense response, increasing the transcription levels of pathogenesis-related proteins (Mori *et al.* 2021), and regulating the gene expression of enzymes for ribosome proteins (Li, Gou, and Li 2019). This is a potential foundation for a deeper understanding of the connection between polarization and protein synthesis in plants.

3.5 Organic carbon content in soil

Organic carbon has a vital role in the function of PMFC as it serves as a nutrient for the microorganisms that aid in plant growth and power generation. Fig. 11 shows the organic carbon

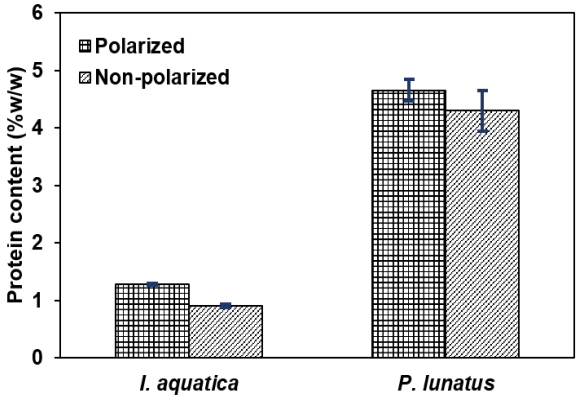

Fig. 10 Protein content of *I. aquatica* and *P. lunatus* leaves

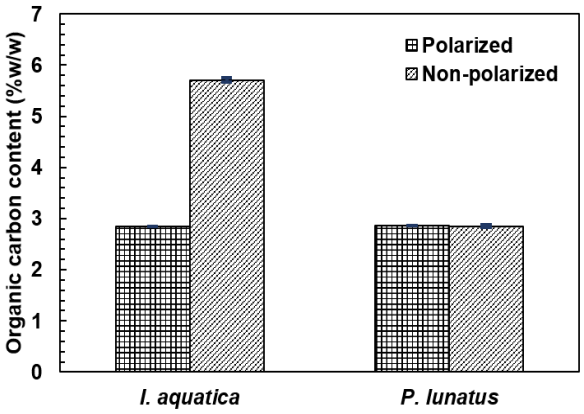

Fig. 11 Organic Carbon content in soil of *I. aquatica* and *P. lunatus*

content in *I. aquatica* and *P. lunatus* soil. It can be seen that the organic carbon content in the soil of *I. aquatica* in PMFC is 50.25% less than that of the control. Meanwhile, there is only a minimal difference for the *P. lunatus*, wherein the PMFC soil is only 0.5% greater than its control counterpart.

For a PMFC to function, anaerobic bacteria consume or oxidize organic matter to proceed with the electron transfer (Karra *et al.* 2013). A study that analyzed organic matter content in PMFC through Chemical Oxygen Demand (COD) measurement concluded that the plant enhances microbial activity (Lin *et al.* 2022) while electrical load enhances organic matter removal rate (Jiang *et al.* 2011), which could have resulted in lower organic carbon content in the soil of *I. aquatica* in PMFC than the control. For the *P. lunatus*, the organic carbon content is almost equal, which is consistent with the findings of an agricultural and bane wood soil polarization study (Dunaj *et al.* 2012).

Nevertheless, the consumption and replenishment of organic carbon is a dynamic process and is not constant all throughout. In most extreme anaerobic conditions, the consumption of organic carbon does not directly proceed to electricity generation; instead, an alternative pathway persists, known as methanogenesis. It utilizes acetate, methanol, methylamines, hydrogen, and carbon dioxide as electron acceptors, producing methane and carbon dioxide (Mobilian and Craft 2022)(Schlesinger and Bernhardt 2020). However, due to its meager energy yield, it is regarded as the final step of organic carbon degradation (Vincent, Jennerjahn, and Ramasamy 2021). Hence, the effect of polarization on organic carbon content in plants is currently inconclusive and requires a more detailed evaluation considering the different degradation pathways.

3.6 Effect of PMFC on soil pH and temperature

Processes involving microorganisms are strict regarding their environmental conditions; they happen at a specific range of pH, temperature, and other parameters. In this study, it was discovered that there is no significant difference in the pH and temperature between the soil in the PMFC and the control. A previous study also yielded the same result, wherein the sediment layer of P-SMFC and their control counterpart both have a pH ranging from 7.5 to 8.0 (Liu *et al.* 2018). Specifically, the pH of the soil in PMFC setups has an average of 6.87 ± 0.26, while the average for the control is 6.87 ± 0.27. It is evident that the pH in the soil in PMFC is only 0.0018 less than the control.

Nevertheless, lower pH values indicate the presence of more root exudates in the soil, which are acidic in nature (Lin *et al.* 2022). Also, the average temperature of the soil in the PMFC

and control is 29.52 ± 1.56 and 29.57 ± 1.53, respectively. This parameter is mainly influenced by ambient conditions, such as air temperature, precipitation, solar radiation, etc. (Yolcubal *et al.* 2004). Since all the setups are exposed to the same environment, the recorded soil temperatures for both PMFC and control vary only by a small amount.

3.7 Voltage and Current in PMFC and SMFC

The produced voltage and current on the *I. aquatica*-powered PMFC (WS-P), *P. lunatus*-powered PMFC (LB-P), and the control counterpart, Soil-MFC (S-C), with and without an external resistance are shown in Figs 12 & 13. For the readings without a resistor, the average voltage produced by WS-P and LB-P throughout the 50-day duration of the experiment were 11.41% and 11.66% higher than the SMFC, respectively, whereas the average current produced by WS-P and LB-P were 129.49% and 164.43% higher than the SMFC, respectively. For the readings against a 1 kΩ resistor, the average voltage produced by WS-P and LB-P were 73.50% and 90.92% higher than the SMFC, respectively, while the average current produced by WS-P and LB-P were 97% and 136.58% higher than the SMFC, respectively.

Based on these values and the time series plots, the PMFCs of *I. aquatica* and *P. lunatus* produced a higher voltage and current than the SMFC. This result is consistent with the findings of previous research that compared the power generation between PMFC and SMFC, using *Spathiphyllum spp* and Vetiver grass (Kwon and Park 2021)(Regmi *et al.* 2018). As previously mentioned, incorporating plants into MFC enhances microbial activity due to rhizodeposition, which could accelerate electron transfer and produce higher energy (Lin *et al.* 2022). It is also evident from the figure that the voltage and current produced by the PMFC were higher without the external

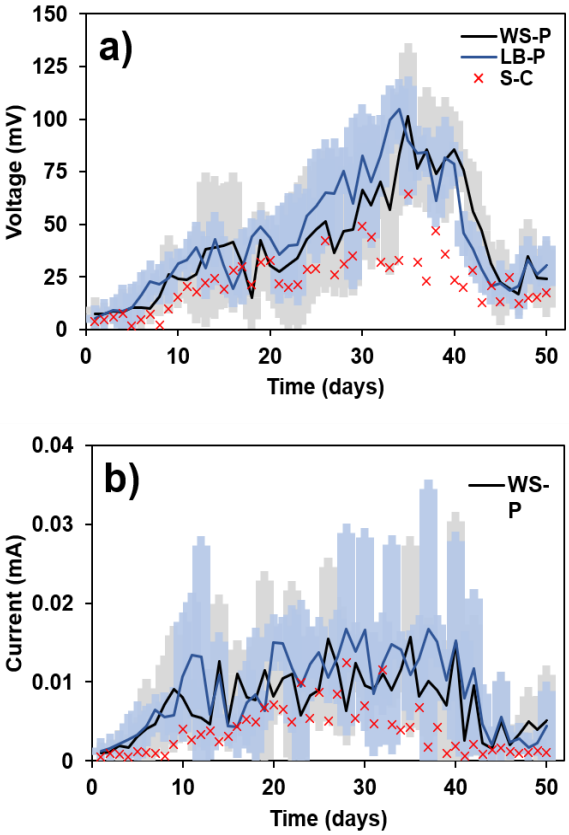

Fig. 13 (a) Voltage and (b) current readings in PMFC and SMFC (control) against a 1 kΩ external resistance

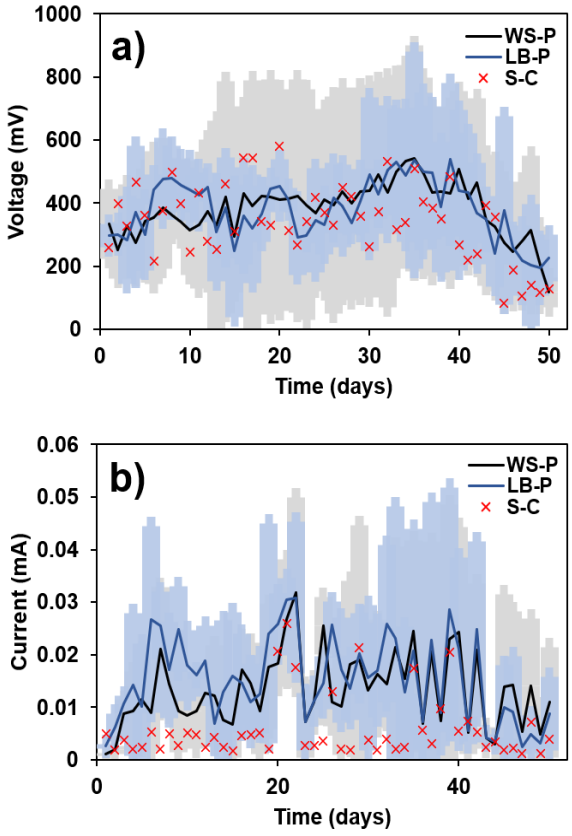

Fig. 12 (a) Voltage and (b) current readings in PMFC and SMFC (control) without external resistance

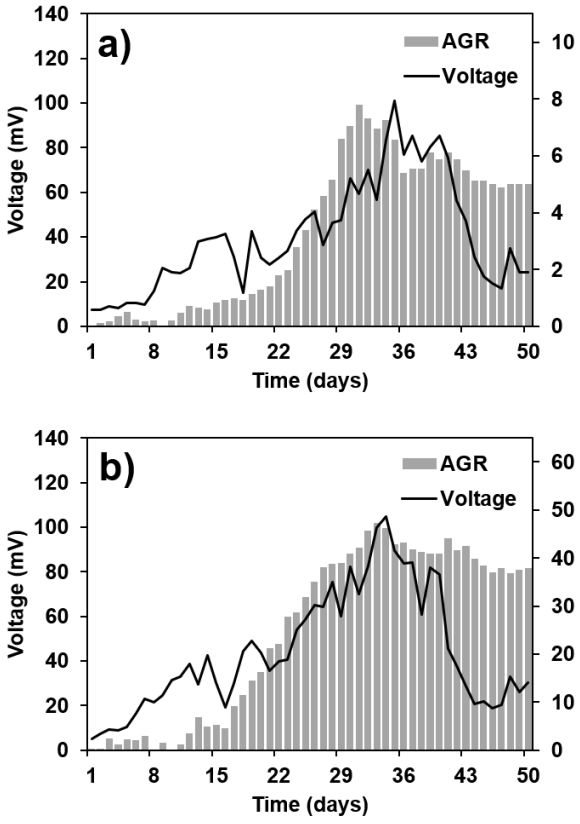

Fig. 14 Average growth rates along voltage readings in (a) *I. aquatica* and (b) *P. lunatus*

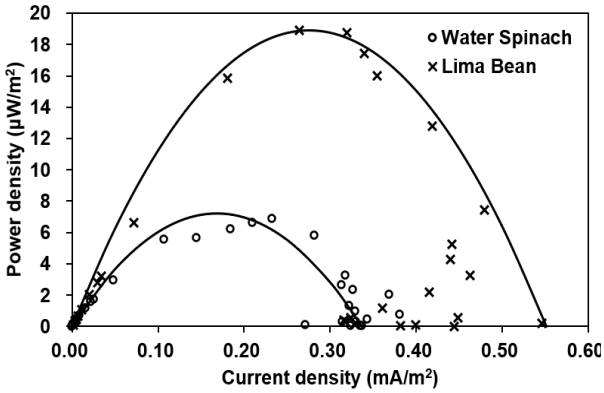

Fig. 15 Response of voltage (a) and current (b) to all studied systems with varying values of resistance

resistance but became more precise when an external resistance was applied as it regulates the flow of the electric current.

Furthermore, the maximum voltage produced by the *I. aquatica* and *P. lunatus* PMFC were 987 mV and 765 mV, which occurred on the 17th and 35th day of the experiment, respectively, whereas the maximum current produced were 61 μA and 54.6 μA, which are both recorded on the 39th day of the experiment. It is also noticeable that the produced voltage and current were decreased in the latter part of the experiment, which could have also been affected by the slowly deteriorating condition of the plant. Fig. 14 shows the average growth rate (AGR), in which a resemblance of the voltage readings can be observed. Other factors that lead to the decrease in power generation are electrode fouling (Jyoti Sarma and Mohanty 2022), an increase in ohmic resistance (Sophia and Sreeja 2017), ambient temperature, and relative humidity (Ma *et al.* 2022).

3.8 Polarization

Fig. 15 shows the polarization curve for *I. aquatica* and *P. lunatus*. Polarization studies performed at the end of the experiment showed that the optimum external resistances in the *I. aquatica* and *P. lunatus*-powered PMFC were 4.7 kΩ and 10 kΩ, respectively. The maximum power density obtained in the *I. aquatica*-powered PMFC was 6.86 μW/m^2, which was 159.02% higher than the power density using the applied external resistance in the experiment (1 kΩ), having a value of 2.65 μW/m^2. Whereas for the *P. lunatus*-powered PMFC, the maximum power density, 18.89 μW/m^2, was 258.69% higher than the power density against 1 kΩ, which is 5.27 μW/m^2.

4. Conclusions

The utilization of the designed 3D-printed plant microbial fuel cells made from PLA-carbon composite conductive filament was found to have a positive impact on the growth of *P. lunatus* and *I. aquatica*. The average daily leaf number and plant height in PMFC for both plants throughout the duration of the experiment were statistically proven to be greater than the control ($\alpha = 0.05$). During harvest, the average final leaf number and plant height for both plants were also higher than the control. This is due to electrostimulation, wherein the electric field energizes the flow of ions in the soil, boosting nutrient uptake and metabolism.

The increase in the microbial community due to the biofilm formation on the anode promoted the root system parameters and the protein content of leaves in the PMFC. The root dry mass of polarized plants was higher by 155.44% and 66.30% for *I. aquatica* and *P. lunatus*, respectively. At the same time, the number of root nodules of the polarized *P. lunatus* was 51.30% higher than its control counterpart. Aside from that, electrostimulation also improved protein synthesis by altering enzyme activity and inducing PR and ribosomal proteins.

The voltage readings resemble the plants' average growth rate, supporting the correlation of plant growth and health to voltage and current production. The polarization studies showed that the optimum external resistances in the *I. aquatica*- and *P. lunatus*-powered PMFC were 4.7 kΩ and 10 kΩ, respectively. Further studies on other soil nutrients and a more extensive analysis of microbial communities in the soil would benefit a deeper understanding of the effect of 3D-printed PMFCs on the root and soil system. The effect of polarization on the organic carbon content in soil is currently inconclusive and still requires further study due to other prevailing pathways of organic carbon consumption.

Acknowledgments

The authors express their gratitude to Mapua University for the support and guidance in accomplishing this study.

Author Contributions: D.P.E.P.: Conceptualization, methodology, experimentation, formal analysis, writing—original draft, K.R.S.P.; writing—review and editing, project administration, validation. All authors have read and agreed to the published version of the manuscript.

Funding: The publication of this research was funded by Mapua University.

Conflicts of Interest: The authors declare no conflict of interest.

References

Agüera, E., & De la Haba, P. 2018. Leaf senescence in response to elevated atmospheric CO_2 concentration and low nitrogen supply. *Biologia Plantarum*, *62*(3), 401–408. https://doi.org/10.1007/s10535-018-0798-z

Arulmani, S. R. B., Gnanamuthu, H. L., Kandasamy, S., Govindarajan, G., Alsehli, M., Elfasakhany, A., Pugazhendhi, A., & Zhang, H. 2021. Sustainable bioelectricity production from Amaranthus viridis and Triticum aestivum mediated plant microbial fuel cells with efficient electrogenic bacteria selections. *Process Biochemistry*, *107*, 27–37. https://doi.org/10.1016/J.PROCBIO.2021.04.015

Bataillou, G., Haddour, N., & Vollaire, C. 2022. Bioelectricity production of PMFC using Lobelia Queen Cardinalis in individual and shared soil configurations. *E3S Web of Conferences*, *334*, 08001. https://doi.org/10.1051/e3sconf/202233408001

Cheng, J., Sun, Z., Li, X., & Yu, Y. 2020. Effects of modified nanoscale carbon black on plant growth, root cellular morphogenesis, and microbial community in cadmium-contaminated soil. *Environmental Science and Pollution Research International*, *27*(15), 18423–18433. https://doi.org/10.1007/S11356-020-08081-Z

Costa, O. Y. A., Raaijmakers, J. M., & Kuramae, E. E. 2018. Microbial extracellular polymeric substances: Ecological function and impact on soil aggregation. *Frontiers in Microbiology*, *9*(JUL), 1–14. https://doi.org/10.3389/fmicb.2018.01636

Dunaj, S. J., Vallino, J. J., Hines, M. E., Gay, M., Kobyljanec, C., & Rooney-Varga, J. N. 2012. Relationships between soil organic matter, nutrients, bacterial community structure, and the performance of microbial fuel cells. *Environmental Science and Technology*, *46*(3), 1914–1922. https://doi.org/10.1021/ES2032532/SUPPL_FILE/ES2032532_SI_001.PDF

Egamberdieva, D., Wirth, S. J., Alqarawi, A. A., Abd-Allah, E. F., & Hashem, A. 2017. Phytohormones and beneficial microbes: Essential components for plants to balance stress and fitness. *Frontiers in Microbiology*, *8*(OCT), 2104. https://doi.org/10.3389/FMICB.2017.02104/BIBTEX

Guan, C. Y., & Yu, C. P. 2021. Evaluation of plant microbial fuel cells for urban green roofs in a subtropical metropolis. *Science of the Total Environment*, *765*, 142786. https://doi.org/10.1016/j.scitotenv.2020.142786

Gude, V. G. 2016. Microbial fuel cells for wastewater treatment and energy generation. *Microbial Electrochemical and Fuel Cells: Fundamentals and Applications*, 247–285. https://doi.org/10.1016/B978-1-78242-375-1.00008-3

Han, Q., Ma, Q., Chen, Y., Tian, B., Xu, L., Bai, Y., Chen, W., & Li, X. 2020. Variation in rhizosphere microbial communities and its association with the symbiotic efficiency of rhizobia in soybean. *ISME Journal*, *14*(8), 1915–1928. https://doi.org/10.1038/s41396-020-0648-9

He, P., Osaki, M., Takebe, M., & Shinano, T. 2003. Comparison of whole system of carbon and nitrogen accumulation between two maize hybrids differing in leaf senescence. *Photosynthetica*, *41*(3), 399–405. https://doi.org/10.1023/B:PHOT.0000015464.27370.60

Hoseinzadeh, E., Wei, C., Farzadkia, M., & Rezaee, A. 2020. Effects of Low Frequency-Low Voltage Alternating Electric Current on Apoptosis Progression in Bioelectrical Reactor Biofilm. *Frontiers in Bioengineering and Biotechnology*, *8*(January), 1–11. https://doi.org/10.3389/fbioe.2020.00002

Huang, X., Duan, C., Duan, W., Sun, F., Cui, H., Zhang, S., & Chen, X. 2021. Role of electrode materials on performance and microbial characteristics in the constructed wetland coupled microbial fuel cell (CW-MFC): A review. *Journal of Cleaner Production*, *301*, 126951. https://doi.org/10.1016/J.JCLEPRO.2021.126951

Imbrogno, F., Assini, S. P., Granata, M., Di Lorenzo, R., & Malcovati, P. 2019. Experimental characterization of the electrical energy produced by microbial fuel cells supplied by pot plants. *2019 IEEE International Workshop on Metrology for Agriculture and Forestry, MetroAgriFor 2019 - Proceedings*, 269–273. https://doi.org/10.1109/METROAGRIFOR.2019.8909234

Jiang, J., Zhao, Q., Wei, L., Wang, K., & Lee, D. J. 2011. Degradation and characteristic changes of organic matter in sewage sludge using microbial fuel cell with ultrasound pretreatment. *Bioresource Technology*, *102*(1), 272–277. https://doi.org/10.1016/j.biortech.2010.04.066

Jyoti Sarma, P., & Mohanty, K. 2022. A novel three-chamber modular PMFC with bentonite/flyash based clay membrane and oxygen reducing biocathode for long term sustainable bioelectricity generation. *Bioelectrochemistry*, *144*, 107996. https://doi.org/10.1016/J.BIOELECHEM.2021.107996

Kabutey, F. T., Zhao, Q., Wei, L., Ding, J., Antwi, P., Quashie, F. K., & Wang, W. 2019. An overview of plant microbial fuel cells (PMFCs): Configurations and applications. *Renewable and Sustainable Energy Reviews*, *110*, 402–414. https://doi.org/10.1016/J.RSER.2019.05.016

Kamali, M., Guo, Y., Aminabhavi, T. M., Abbassi, R., Dewil, R., & Appels, L. 2023. Pathway towards the commercialization of sustainable microbial fuel cell-based wastewater treatment technologies. *Renewable and Sustainable Energy Reviews*, *173*(December 2022), 113095. https://doi.org/10.1016/j.rser.2022.113095

Karamzadeh, M., Kadivarian, H., Kadivarian, M., & Kazemi, A. 2020. Modeling the influence of substrate concentration, anode electrode surface area and external resistance in a start-up on the performance of microbial fuel cell. *Bioresource Technology Reports*, *12*, 100559. https://doi.org/10.1016/J.BITEB.2020.100559

Karra, U., Manickam, S. S., McCutcheon, J. R., Patel, N., & Li, B. 2013. Power generation and organics removal from wastewater using activated carbon nanofiber (ACNF) microbial fuel cells (MFCs). *International Journal of Hydrogen Energy*, *38*(3), 1588–1597. https://doi.org/10.1016/J.IJHYDENE.2012.11.005

Kumar, V., Khare, T., Srivastav, A., Surekha, C., Shriram, V., & Wani, S. H. 2018. Oxidative stress and leaf senescence: Important insights. In *Senescence Signalling and Control in Plants*. Elsevier Inc. https://doi.org/10.1016/B978-0-12-813187-9.00009-3

Kwon, K. J., & Park, B. J. 2021. Efficiency of Spathiphyllum spp. as a plant-microbial fuel cell. *Ornamental Horticulture*, *27*(2), 173–182. https://doi.org/10.1590/2447-536X.V27I2.2264

Li, Z. G., Gou, H. Q., & Li, R. Q. 2019. Electrical stimulation boosts seed germination, seedling growth, and thermotolerance improvement in maize (Zea mays L.). *Plant Signaling and Behavior*, *14*(12). https://doi.org/10.1080/15592324.2019.1681101

Lim, P. O., & Nam, H. G. 2005. The Molecular and Genetic Control of Leaf Senescence and Longevity in Arabidopsis. In *Current Topics in Developmental Biology* (Vol. 67, Issue 04). Elsevier Masson SAS. https://doi.org/10.1016/S0070-2153(05)67002-0

Lin, C. W., Alfanti, L. K., Cheng, Y. S., & Liu, S. H. 2022. Enhancing bioelectricity production and copper remediation in constructed single-medium plant sediment microbial fuel cells. *Desalination*, *542*, 116079. https://doi.org/10.1016/J.DESAL.2022.116079

Liu, Y., Zhang, H., Lu, Z., de Lourdes Mendoza, M., Ma, J., Cai, L., & Zhang, L. 2018. Decreasing sulfide in sediment and promoting plant growth by plant–sediment microbial fuel cells with emerged plants. *Paddy and Water Environment 2018 17:1*, *17*(1), 13–21. https://doi.org/10.1007/S10333-018-0679-2

Lu, Z., Yin, D., Chen, P., Wang, H., Yang, Y., Huang, G., Cai, L., & Zhang, L. 2020. Power-generating trees: Direct bioelectricity production from plants with microbial fuel cells. *Applied Energy*, *268*(October 2019), 115040. https://doi.org/10.1016/j.apenergy.2020.115040

Ma, J., Zhang, C., Xi, F., Chen, W., Jiao, K., Du, Q., Bai, F., & Liu, Z. 2022. Experimental study on the influence of environment conditions on the performance of paper-based microfluidic fuel cell. *Applied Thermal Engineering*, 119487. https://doi.org/10.1016/J.APPLTHERMALENG.2022.119487

Maddalwar, S., Kumar Nayak, K., Kumar, M., & Singh, L. 2021. Plant microbial fuel cell: Opportunities, challenges, and prospects. *Bioresource Technology*, *341*, 125772. https://doi.org/10.1016/J.BIORTECH.2021.125772

Matassa, S., Boon, N., Pikaar, I., & Verstraete, W. 2016. Microbial protein: future sustainable food supply route with low environmental footprint. *Microbial Biotechnology*, *9*(5), 568. https://doi.org/10.1111/1751-7915.12369

Mobilian, C., & Craft, C. B. 2022. Wetland Soils: Physical and Chemical Properties and Biogeochemical Processes. In *Encyclopedia of Inland Waters* (2nd ed., Vol. 3, pp. 157–168). Elsevier. https://doi.org/10.1016/B978-0-12-819166-8.00049-9

Morales, C., Solís, S., Bacame-Valenzuela, F. J., Reyes-Vidal, Y., Cárdenas, J., Manríquez, J., & Bustos, E. 2021. Electrical stimulation of Cucumis sativus in an Antrosol using modified electrodes with transition metal oxides at the in situ pilot level. *Journal of Electroanalytical Chemistry*, *895*(June), 115528. https://doi.org/10.1016/j.jelechem.2021.115528

Mori, D., Moriyama, A., Kanamaru, H., Aoki, Y., Masumura, Y., & Suzuki, S. 2021. Electrical stimulation enhances plant defense response in grapevine through salicylic acid-dependent defense pathway. *Plants*, *10*(7), 1–10. https://doi.org/10.3390/plants10071316

Narayana Prasad, P., & Kalla, S. 2021. Plant-microbial fuel cells - A bibliometric analysis. *Process Biochemistry*, *111*, 250–260. https://doi.org/10.1016/J.PROCBIO.2021.10.001

Nitisoravut, R., & Regmi, R. 2017. Plant microbial fuel cells: A promising biosystems engineering. *Renewable and Sustainable Energy Reviews*, *76*, 81–89. https://doi.org/10.1016/J.RSER.2017.03.064

Nogué, F., Gonneau, M., & Faure, J.-D. 2003. Cytokinins. In *Encyclopedia of Hormones* (pp. 371–378). https://doi.org/10.1016/B0-12-341103-3/00061-9

Omar, M. H., Razak, K. A., Ab Wahab, M. N., & Hamzah, H. H. 2021. Recent progress of conductive 3D-printed electrodes based upon polymers/carbon nanomaterials using a fused deposition modelling (FDM) method as emerging electrochemical sensing devices. *RSC Advances*, *11*(27), 16557–16571. https://doi.org/10.1039/d1ra01987b

Peng, T., Kellens, K., Tang, R., Chen, C., & Chen, G. 2018. Sustainability of additive manufacturing: An overview on its energy demand

and environmental impact. *Additive Manufacturing*, *21*, 694–704. https://doi.org/10.1016/J.ADDMA.2018.04.022

Regmi, R., Nitisoravut, R., Charoenroongtavee, S., Yimkhaophong, W., & Phanthurat, O. 2018. Earthen Pot–Plant Microbial Fuel Cell Powered by Vetiver for Bioelectricity Production and Wastewater Treatment. *CLEAN – Soil, Air, Water*, *46*(3), 1700193. https://doi.org/10.1002/CLEN.201700193

Rocha, R. G., Ramos, D. L. O., de Faria, L. V., Germscheidt, R. L., dos Santos, D. P., Bonacin, J. A., Munoz, R. A. A., & Richter, E. M. 2022. Printing parameters affect the electrochemical performance of 3D-printed carbon electrodes obtained by fused deposition modeling. *Journal of Electroanalytical Chemistry*, 116910. https://doi.org/10.1016/J.JELECHEM.2022.116910

Roy Choudhury, S., Johns, S. M., & Pandey, S. 2019. A convenient, soil-free method for the production of root nodules in soybean to study the effects of exogenous additives. *Plant Direct*, *3*(4), 1–11. https://doi.org/10.1002/PLD3.135

Sarma, P. J., & Mohanty, K. 2023. Development and comprehensive characterization of low-cost hybrid clay based ceramic membrane for power enhancement in plant based microbial fuel cells (PMFCs). *Materials Chemistry and Physics*, *296*, 127337. https://doi.org/10.1016/j.matchemphys.2023.127337

Schlesinger, W. H., & Bernhardt, E. S. 2020. Wetland Ecosystems. In *Biogeochemistry* (4th ed., pp. 249–291). Academic Press. https://doi.org/10.1016/B978-0-12-814608-8.00007-4

Shamsi, I. H., Sagonda, T., Zhang, X., Zvobgo, G., & Joan, H. I. 2018. The role of growth regulators in senescence. In *Senescence Signalling and Control in Plants*. Elsevier Inc. https://doi.org/10.1016/B978-0-12-813187-9.00006-8

Sharma, S., & Agarwal, S. K. 2018. Plant leaf senescence: integrating multiple environmental and internal cues. In *Senescence Signalling and Control in Plants*. Elsevier Inc. https://doi.org/10.1016/B978-0-12-813187-9.00003-2

Slate, A. J., Hickey, N. A., Butler, J. A., Wilson, D., Liauw, C. M., Banks, C. E., & Whitehead, K. A. 2021. Additive manufactured graphene-based electrodes exhibit beneficial performances in Pseudomonas aeruginosa microbial fuel cells. *Journal of Power Sources*, *499*, 229938. https://doi.org/10.1016/J.JPOWSOUR.2021.229938

Sophia, A. C., & Sreeja, S. 2017. Green energy generation from plant microbial fuel cells (PMFC) using compost and a novel clay separator. *Sustainable Energy Technologies and Assessments*, *21*, 59–66. https://doi.org/10.1016/J.SETA.2017.05.001

Vincent, S. G. T., Jennerjahn, T., & Ramasamy, K. 2021. Environmental variables and factors regulating microbial structure and functions. In *Microbial Communities in Coastal Sediments* (pp. 79–117). Elsevier. https://doi.org/10.1016/B978-0-12-815165-5.00003-0

Wang, C., Zhang, H., Ren, D., Li, Q., Zhang, S., & Feng, T. 2015. Effect of Direct-Current Electric Field on Enzymatic Activity and the Concentration of Laccase. *Indian Journal of Microbiology*, *55*(3), 278–284. https://doi.org/10.1007/s12088-015-0523-y

Wang, H., Gu, C., Liu, X., Yang, C., Li, W., & Wang, S. 2020. Impact of Soybean Nodulation Phenotypes and Nitrogen Fertilizer Levels on the Rhizosphere Bacterial Community. *Frontiers in Microbiology*, *11*(May), 1–10. https://doi.org/10.3389/fmicb.2020.00750

Wang, Q., Liu, J., & Zhu, H. 2018. Genetic and molecular mechanisms underlying symbiotic specificity in legume-rhizobium interactions. *Frontiers in Plant Science*, *9*, 313. https://doi.org/10.3389/FPLS.2018.00313/BIBTEX

Winfield, J., Gajda, I., Greenman, J., & Ieropoulos, I. 2016. A review into the use of ceramics in microbial fuel cells. *Bioresource Technology*, *215*, 296–303. https://doi.org/10.1016/J.BIORTECH.2016.03.135

Wouters, P. C., Dutreux, N., Smelt, J. P. P. M., & Lelieveld, H. L. M. 1999. Effects of pulsed electric fields on inactivation kinetics of Listeria innocua. *Applied and Environmental Microbiology*, *65*(12), 5364–5371. https://doi.org/10.1128/AEM.65.12.5364-5371.1999

Yamaguchi, I., Cohen, J. D., Culler, A. H., Quint, M., Slovin, J. P., Nakajima, M., & Sakagami, Y. 2010. Plant Hormones. In *Comprehensive Natural Products II* (Vol. 4, pp. 9–125). https://doi.org/10.1016/B978-008045382-8.00092-7

Yi, J. Y., Choi, J. W., Jeon, B. Y., Jung, I. L., & Park, D. H. 2012. Effects of a low-voltage electric pulse charged to culture soil on plant growth and variations of the bacterial community. *Agricultural Sciences*, *2012*(03), 339–346. https://doi.org/10.4236/AS.2012.33038

Yolcubal, I., Brusseau, M. L., Artiola, J. F., Wierenga, P. J., & Wilson, L. G. 2004. ENVIRONMENTAL PHYSICAL PROPERTIES AND PROCESSES. *Environmental Monitoring and Characterization*, 207–239. https://doi.org/10.1016/B978-012064477-3/50014-X

Yoneyama, K., & Natsume, M. 2010. Allelochemicals for Plant–Plant and Plant–Microbe Interactions. *Comprehensive Natural Products II: Chemistry and Biology*, *4*, 539–561. https://doi.org/10.1016/B978-008045382-8.00105-2

You, J., Preen, R. J., Bull, L., Greenman, J., & Ieropoulos, I. 2017. 3D printed components of microbial fuel cells: Towards monolithic microbial fuel cell fabrication using additive layer manufacturing. *Sustainable Energy Technologies and Assessments*, *19*, 94–101. https://doi.org/10.1016/j.seta.2016.11.006

Zhang, W., Zhang, F., Niu, Y., Li, Y. X., Jiang, Y., Bai, Y. N., Dai, K., & Zeng, R. J. 2020. Power to hydrogen-oxidizing bacteria: Effect of current density on bacterial activity and community spectra. *Journal of Cleaner Production*, *263*, 121596. https://doi.org/10.1016/J.JCLEPRO.2020.121596

Zhao, F., Xin, X., Cao, Y., Su, D., Ji, P., Zhu, Z., & He, Z. 2021. Use of Carbon Nanoparticles to Improve Soil Fertility, Crop Growth and Nutrient Uptake by Corn (Zea mays L.). *Nanomaterials 2021*,11(10), 2717. https://doi.org/10.3390/NANO11102717

Zhou, E., Lekbach, Y., Gu, T., & Xu, D. 2022. Bioenergetics and extracellular electron transfer in microbial fuel cells and microbial corrosion. *Current Opinion in Electrochemistry*, *31*, 100830. https://doi.org/10.1016/J.COELEC.2021.100830